Estimation of Metabolite Concentrations from Localized *in Vivo* Proton NMR Spectra

Stephen W. Provencher

The LCModel method analyzes an *in vivo* spectrum as a *L*inear *C*ombination of *Model* spectra of metabolite solutions *in vitro*. By using complete model spectra, rather than just individual resonances, maximum information and uniqueness are incorporated into the analysis. A constrained regularization method accounts for differences in phase, baseline, and lineshapes between the *in vitro* and *in vivo* spectra, and estimates the metabolite concentrations and their uncertainties. LCModel is fully automatic in that the only input is the time-domain *in vivo* data. The lack of subjective interaction should help the exchange and comparison of results. More than 3000 human brain STEAM spectra from patients and healthy volunteers have been analyzed with LCModel. *N*-acetylaspartate, cholines, creatines, *myo*-inositol, and glutamate can be reliably determined, and abnormal levels of these or elevated levels of lactate, alanine, *scyllo*-inositol, glutamine, or glucose clearly indicate numerous pathologies. A computer program will be available.

Key words: NMR; spectroscopy; quantification; *in vivo*.

INTRODUCTION

Recent significant improvements in localization and in the quality of ^{1}H NMR spectra *in vivo* could open up important new ways for clinical diagnoses and for *in vivo* biochemical studies. For example, stimulated echo (STEAM) localization sequences with short echo times (1) show many metabolites in the human brain (2).

If these methods are to be fully exploited, the objective and reliable determination of the metabolites and their concentrations is essential. The classical approaches, from high-resolution NMR *in vitro*, of integrating single peaks interactively or with a computer fit to a specified lineshape are unreliable with localized *in vivo* spectra for many reasons. For example, eddy currents and inhomogeneities in field and environment cause complicated line broadening and peak overlap. There is also a large unknown background ("baseline") from the vast majority of protons that are not accounted for in the analysis, particularly in the more informative spectra using short echo times. At the relatively low field strengths currently used with humans, strong spin-spin coupling also complicates the use of multiplet peaks. Even without serious baseline and low-field problems, De Graaf and Bovée (3) showed that single-peak analyses of relatively low-resolution spectra were unreliable and that extra constraints on the separations and relative amplitudes of the resonances of the individual metabolites had to be introduced to get useful estimates.

In this paper the LCModel method is presented. It analyzes the *in vivo* spectrum as a linear combination of a basis set of complete model spectra of metabolite solutions *in vitro* (4). By using complete spectra, rather than just individual peaks, full use is made of the information in the spectra. Their complexities (high information content) now become advantageous, because two metabolites with overlapping peaks at one chemical shift can still be separated if their spectra are different at other chemical shifts. By using the same protocol for the model *in vitro* spectra as for the *in vivo* spectra, complications from the localization sequence, spin-spin couplings, etc. are automatically accounted for. The method is not restricted to a particular localization method or field strength. A similar strategy is now widely used in the analysis of protein circular dichroism spectra (5), which have high complexity but low resolution.

A major problem with the quantification of *in vivo* spectra has been parameterized models for peak distortion and for the baseline, which are too complicated to specify *a priori*. Empirical models with too few parameters introduce bias. Too many parameters produce artifacts and instabilities in the analysis. Both situations cause errors in the estimates. LCModel uses a nearly model-free constrained regularization method (6), which attempts to choose the best compromise between these two situations by finding the smoothest lineshape and baseline consistent with the data.

Another major problem has been user subjectivity and bias, which hinders the exchange of results within and between laboratories. LCModel is fully automatic in that the only necessary input is the time-domain *in vivo* data; there is no user interaction. The method is outlined in the next section, and specified in the Appendix.

The final sections summarize the possibilities and limitations and give guidelines on the minimum usable spectral quality, particularly the resolution. Experience and examples from user analyses of 3451 human brain STEAM spectra with LCModel are used. Only concentration ratios are discussed here, since the spectra were measured over 3 years under varying conditions. However, recent results (7) indicate that under more uniform conditions the spectra can be scaled to yield absolute concentrations, and LCModel does this.

MRM 30:672–679 (1993)

From the Max-Planck-Institut für biophysikalische Chemie, Göttingen, Federal Republic of Germany.

Address correspondence to: Stephen W. Provencher, Ph.D., Max-Planck-Institut für biophysikalische Chemie, Postfach 2841, D-37018 Göttingen, Federal Republic of Germany.

Received May 10, 1993; revised August 6, 1993; accepted August 6, 1993.

A preliminary report of this work was presented at the 11th Annual Meeting of the Society of Magnetic Resonance in Medicine, held in Berlin, FRG, August 1992.

0740-3194/93 $3.00

Table 1
Variability of Estimated Metabolite Concentration Ratios in Human Brain[a]

Metabolite[b]	1 Adult (TR = 3 s)	26 Adults (TR = 6 s)	
	gm (N = 14)[c]	gm (N = 26)	wm (N = 40)
NAA+NAAG	1.32 ± 3%	1.34 ± 7%	1.74 ± 11%
Cr+PCr	1.0	1.0	1.0
NAA	1.29 ± 6%	1.30 ± 6%	1.44 ± 9%
Cho	0.19 ± 7%	0.18 ± 10%	0.29 ± 14%
Lac	0.07 ± 57%	0.08 ± 83%	0.12 ± 67%
Ala	0.006 ± 374%	0.005 ± 214%	0.03 ± 168%
myo-Inositol	0.78 ± 5%	0.68 ± 9%	0.63 ± 19%
Glu	1.23 ± 9%	1.26 ± 10%	0.98 ± 17%
scyllo-Ins	0.03 ± 30%	0.02 ± 64%	0.02 ± 101%
Gln	0.49 ± 20%	0.55 ± 19%	0.37 ± 43%
NAAG	0.03 ± 167%	0.03 ± 148%	0.31 ± 42%
Asp	0.17 ± 36%	0.26 ± 29%	0.08 ± 138%
Glucose	(infused)	0.12 ± 56%	0.03 ± 192%
GABA	0.15 ± 67%	0.17 ± 47%	0.16 ± 104%
Taurine	0.50 ± 18%	0.59 ± 16%	0.45 ± 53%

[a] All concentrations are ratios to the total Cr + PCr. The values are means ± %SD, where %SD = 100 × SD/mean. No corrections were made for TE = 20 ms or finite TR.
[b] *N*-Acetylaspartate (NAA), *N*-Acetylaspartylglutamate (NAAG), Creatine (Cr), Phosphocreatine (PCr), Cholines (Cho), Lactate (Lac), Alanine (Ala), Glutamate (Glu), *scyllo*-Inositol (*scyllo*-Ins), Glutamine (Gln), Aspartate (Asp), γ-Aminobutyric Acid (GABA).
[c] N = number of spectra used for the mean, either from parietal gray matter (gm) or parietal white matter (wm).

METHOD

Basis Set of Model *in Vitro* Spectra

The noise level in the model spectra in the basis set should be small compared with that in the *in vivo* spectra. This is usually easy to realize *in vitro* with higher concentrations and more scans (as long as frequency drifts remain small). This should avoid the necessity of a further refinement of the model spectra by smoothing or fitting to theoretical models, which would have to be done very carefully to avoid bias.

The basis set can be used to analyze any *in vivo* spectrum acquired with the same protocol. The only conditions that can vary among the *in vivo* spectra, are those, such as the volume-of-interest (VOI), that only scale the metabolite spectra by constants, but do not otherwise change their structure. One high-quality basis set shared by many groups using the same field strength and protocol would greatly improve the exchange of results, but variations among instruments might require individual basis sets.

The examples shown here used a basis set of model spectra from solutions of 15 metabolites (listed in Table 1). The model spectra were acquired at 2.0 T in a spherical phantom with a volume of 250 ml using three CHESS cycles for water suppression followed by a STEAM localization sequence with an echo time of TE = 20 ms, a 30 ms middle interval, a repetition time of TR = 6 s, and 2048 data points with a dwell time of 0.5 ms. Other details are given in ref. 2, except that, to preserve information, no gaussian filter was applied to any data. This basis set was used for all 3451 *in vivo* spectra.

The model spectra are not distorted by strong baseline or field inhomogeneity effects, and conventional interactive phasing and referencing is no problem. Any reference peaks, such as from acetate or glycine, are replaced with an interpolated baseline. It would be better to avoid this complication by using a reference compound with resonances outside of the spectral window used in the analysis (e.g., below 1.0 ppm).

The model (as well as the *in vivo*) spectra are scaled together by multiplying each spectrum by the transmitter amplitude of a nonselective 90° RF pulse of 0.5 ms duration (7) and by dividing by the VOI. The model spectra are normalized by dividing by their concentrations.

Analysis

The *in vivo* spectrum is analyzed as a linear combination of the model *in vitro* spectra, which are modified to account for the following differences between *in vitro* and *in vivo*: a) for each model spectrum in the basis set, T_2 broadening and a small frequency shift due to possible referencing errors, b) for the whole basis set, a convolution due to field inhomogeneities, eddy currents, frequency drifts, etc., c) a baseline, and d) zero- and first-order phase corrections for the *in vivo* spectrum. A constrained regularization method for the convolution and baseline makes them nearly model-free. A constrained nonlinear least-squares analysis estimates the metabolite concentrations and their uncertainties. LC-Model is described in more detail in the Appendix.

RESULTS AND DISCUSSION

Normal Spectra

Preliminary test analyses of known mixtures of metabolites *in vitro* were accurate (4). For example, a 50 mM equimolar mixture of NAA, Glu, and Gln yielded concentration ratios of 1:1.01:1.03, and a 1:1:0 mixture

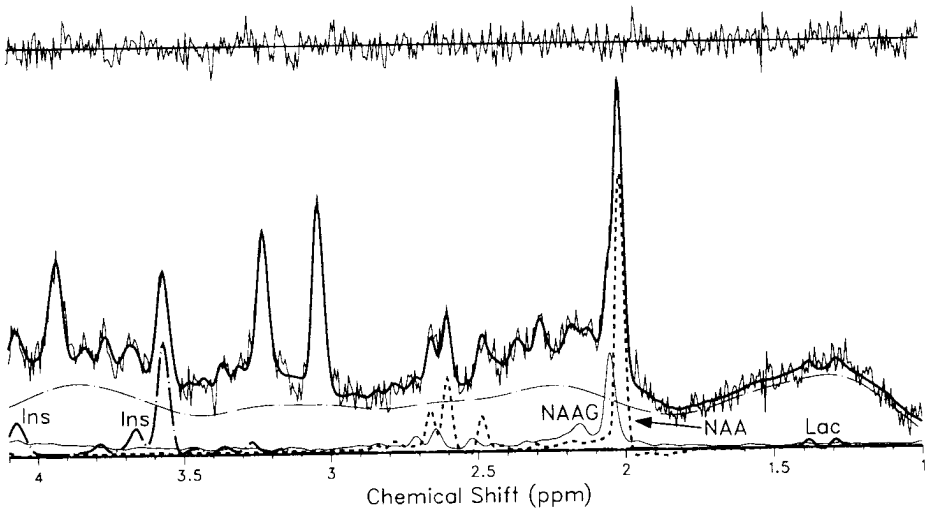

FIG. 1. LCModel analysis (thick curve) of one of the white matter spectra (thin curve) used for Table 1, with a linewidth (FWHM) of about 0.04 ppm. The differences (residuals) between these two are plotted above, and appear quite randomly scattered, indicating a fit to within experimental error. Also shown are the contributions of NAA, NAAG, *myo*-inositol (Ins), Lac, and the baseline (thin broken curve). NAA and NAAG can be reliably resolved.

yielded 1:0.97:0.02. Concentrations of the other metabolites were small with large estimated relative uncertainties. This verified the algorithm, but tests with *in vivo* spectra with realistic resolution, baseline distortions, and signal/noise ratios were necessary. All 3451 available *in vivo* spectra, regardless of quality, were analyzed with only the time-domain data as input.

Table 1 shows the variability in the analyses of spectra under two sets of conditions. The left columns represent nearly ideal conditions, where the spectra were acquired during a glucose infusion experiment with all other conditions kept constant, including the 18 ml VOI and 128 scans. Here the error estimates from LCModel agree very well with the observed scatter (%SD), which is mainly due to random noise. The scatter for the major metabolites is remarkably small. Although there is an important additional uncertainty factor in the absolute concentrations, the high internal precision of LCModel should be useful in such physiological studies or in clinical comparisons with controls obtained under similar conditions.

The right columns of Table 1 reflect the more common situation in clinical practice, where there is additional variability of measuring conditions, spectral quality, and subjects (26 young healthy adults). In addition, the signal/noise ratio was worse, because usually only 64 scans were done, and the VOI range was 8 to 18 ml in gray matter and 8 to 12 ml in white matter. Nevertheless, the precision for the major metabolites seems more than adequate for many purposes.

Using criteria described below, the rows of Table 1 are listed roughly in order of decreasing reliability. Separate spectra of PCr and Cr are in the basis set, but they are not listed separately in Table 1, because their correlation coefficient (output by LCModel) is stronger than −0.9. This indicates that they are only resolved from each other with very large uncertainties. However, the sum Cr+PCr is very well determined. Furthermore, the correlation coefficient of the sum Cr+PCr with other metabolites (except GABA) is usually positive, indicating that the other metabolites tend to have fluctuations of the same sign as Cr+PCr (probably mainly due to fluctuations in the baseline). Thus, it is reasonable to form ratios of concentrations relative to Cr+PCr, as in Table 1.

NAA and NAAG also have a strong negative correlation coefficient, and the sum NAA+NAAG is much more

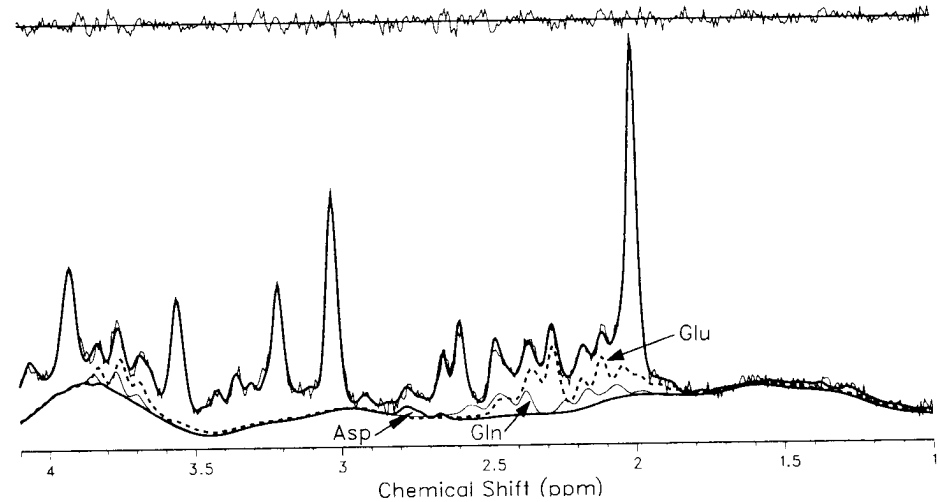

FIG. 2. LCModel analysis of one of the best gray matter spectra used for Table 1, with FWHM ≈ 0.04 ppm. Conventions are as for Fig. 1, except that the baseline has been included in the contributions of Glu, Gln, and Asp.

reliable than NAAG alone. However, Table 1 shows that NAAG can still be reliably detected in adult white matter. This can also be seen in Fig. 1, where a spectrum with relatively high resolution and signal/noise ratio (128 scans and VOI = 8 ml) is shown.

Another problem pair in the past, Glu and Gln, usually have a positive correlation coefficient. Thus, somewhat surprisingly, the main source of uncertainty is not the similarity of their spectra but rather the baseline. The Gln/Glu ratio is a useful quantity; its %SD (not shown) is about that of the Gln/Cr+PCr ratio. The contributions of Gln, Glu, and Asp to one of the best spectra used for Table 1 (128 scans, VOI = 18 ml, TR = 6 s) is shown in Fig. 2. Gln and Asp clearly have larger uncertainties than Glu. They would be difficult to quantify with single-peak integration methods. However, it is still possible to see indications in Table 1 of more Asp (as well as Glu) in gray matter than in white matter, but about the same total NAA+NAAG+Asp in gray and white matter. These indications are strengthened by accounting for partial-volume effects (7) and the Cr+PCr gray/white-matter ratio of 1.1 (not shown).

The large %SD values for many of the metabolites in Table 1 show that they are barely detectable in normal cases. However, reliable estimates of elevated levels of Lac, Ala, *Scyllo*-Ins, Gln, or glucose are obtained and clearly indicate numerous pathological cases. For example, LCModel shows the smooth rise and fall of brain glucose in infusion experiments such as that used for Table 1 (J. Frahm *et al.*, to be published).

Peak Distortions

It is essential to have a reliable, nearly model-independent method for correcting for the unpredictable peak distortions that occur *in vivo*. The lineshape coefficients, S_n, in Eq. [1] in the Appendix account for peak distortions that are convolutions in the frequency domain. These include effects from field inhomogeneities and, to a good approximation (8), residual eddy currents. Since LCModel uses all the lines in the spectral window to determine the S_n, they are quite reliable. This is best illustrated with the unusually extreme case in Fig. 3. Usually the S_n in Fig. 3A form a smooth unimodal profile to account for field inhomogeneity, but here they also account for extreme eddy-current effects.

Figure 3C shows the LCModel fit after the same time-domain data were first corrected for eddy-current effects using the method of Klose (9) (implemented in the routine ECC, Siemens, Erlangen). The concentration ratios (not shown) from the analyses in Figs. 3B and 3C agree fairly well. However, in such extreme cases, it is obviously best to repeat the measurement, or at least to apply the Klose correction, especially if absolute concentrations are sought. Preliminary results indicate that it is very beneficial to make the Klose correction an integral part of the protocol. It requires a reference spectrum without water suppression, but a single scan seems adequate, and the correction is very simple to implement.

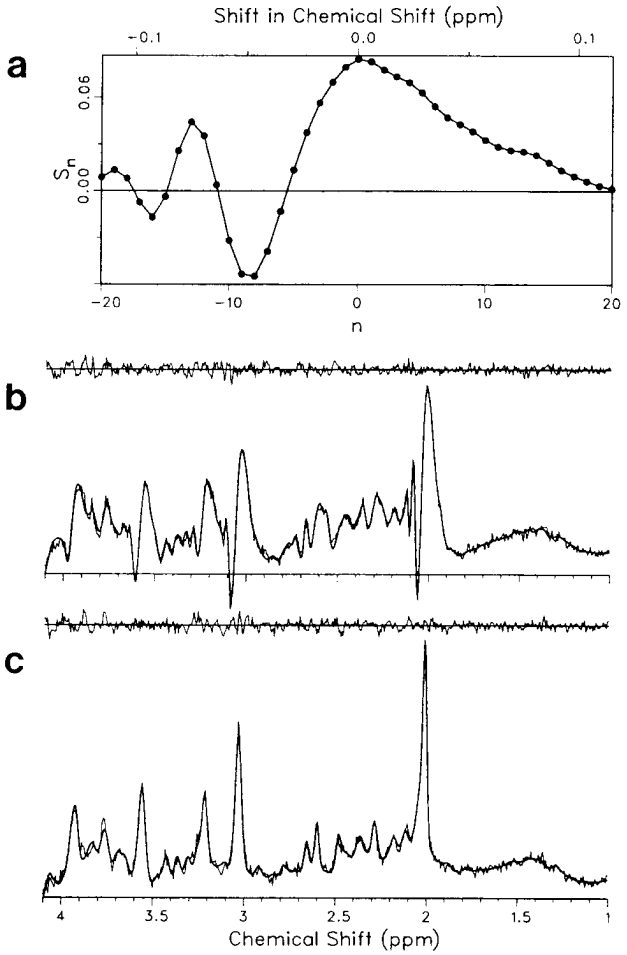

FIG. 3. (a) The lineshape coefficients, S_n in Eq. [1], can still account for the extreme peak distortions in the spectrum in (b). (c) Spectrum and LCModel fit after the same time-domain data for (b) were first corrected for eddy-current effects by the Klose method (9). The FWHM ≈ 0.03 ppm in (c) and 0.07 ppm for the main lobe in (a) and (b). The conventions for the curves in (b) and (c) are as in Fig. 1.

Fundamental Uniqueness Limitations

Every spectrum has a degree of nonuniqueness in that there is a range (confidence region) of metabolite concentrations and other parameters that all fit the data to within experimental error. Without more data or prior information to restrict the model, it is impossible to reliably choose the correct solution from this set of feasible solutions, regardless of the data analysis method used. Thus, the uniqueness limitations discussed in this section are fundamental to the experimental method and not restricted to LCModel.

The two main sources of nonuniqueness are the baseline and low spectral resolution. With TE = 20 ms, the integrated baseline is typically as large as the contributions of the metabolite spectra in the basis set. Thus, 50% of the spectrum is unaccounted for by the basis set, not counting invisible immobilized components.

The baseline becomes a serious problem when the

spectral resolution is low. In Fig. 4, the usually well-defined doublets of Ala and Lac are no longer resolved, and they fill in the hump in the range 1.6 to 1.2 ppm to within experimental error. Without further information or bias, it is impossible to decide whether this hump is really Ala and Lac or baseline. At normal resolution, the Lac and Ala doublets cannot be easily confused with the commonly occurring hump in their region. In Fig. 1, only a 0.08 ratio of Lac to Cr+PCr is found with an estimated 62% relative uncertainty, indicating that it is practically indistinguishable from the noise. Lac and Ala can be reliably estimated with the resolution in Fig. 1, but not in Fig. 4.

In Fig. 4, the correlation coefficient between Glu and Gln has become negative, and it is clearly more difficult to resolve Gln from Glu than in Fig. 2. The large area between the Glu (plus baseline) curve in Fig. 4 and the total fit is filled with (strongly overlapping) peaks from other metabolites. Thus, the peak-overlap problem is much worse in Fig. 4 than in Fig. 2, where the area between Glu plus baseline and the total fit is much smaller. The reliability obviously rapidly deteriorates with decreasing resolution.

Normally the zero- and first-order phase corrections are well-determined. However, low resolution combined with the lack of strong landmarks such as NAA, Cr+PCr, and Cho (as in cerebrospinal fluid) can result in a wide range of phase corrections that all fit the data to within experimental error. This occurred (and was clearly indicated) in about 0.5% of the analyses.

Ranking the Reliabilities

The metabolites in Table 1 are ordered roughly according to their robustness to the baseline and spectral resolution. This is subjective because the %SD depends on concentration. Experience with the 3451 analyses, particularly elevated concentrations in pathological cases, was used for this ranking. Taurine is the worst; with decreasing resolution, its apparent quartet quickly coalesces to one broad hump with little structure, and this can be easily confused with baseline plus noise and *vice versa*. Other metabolites in Table 1 also have coalescing multiplets, but they form two or more humps that remain well-separated from each other. Since LCModel uses the complete model spectrum, information on the positions, structures, and relative areas of each of these humps is automatically imposed, and this helps to preserve uniqueness. NAA+NAAG and Cr+PCr are best because they each have well separated structures plus strong singlets that cannot be easily confused with the baseline. The concentrations of NAA+NAAG and Cr+PCr from the analysis in Fig. 4 still have low estimated uncertainties, even at this poor resolution.

Basis Set

Another criterion for the ranking in Table 1 was to remove one of the metabolites from the basis set (4). When a metabolite high in Table 1 is removed, its absence tends to be clearly indicated by a poor fit in the parts of the spectrum where it normally occurs (provided that it is present at significant concentration to begin with). When a metabolite low in Table 1 is removed, it can be better compensated by the baseline and small adjustments to other metabolite concentrations.

Good estimates for metabolites high in Table 1 can often still be obtained when metabolites low in Table 1 are removed from the basis set. However, there is no reason to do this. In general, a metabolite that has a good possibility of being detected should be included in the basis set. Even highly correlated pairs, such as Cr and PCr, do not harm the analysis. Error estimates and correlation coefficients for Cr, PCr, and the sum Cr+PCr clearly show that only the Cr+PCr concentration is reliable.

The basis set in Table 1 was sufficient to fit nearly all of the spectra, including 1868 patient spectra. This indicates that most other metabolites unfortunately do not contribute uniquely enough to the *in vivo* spectra to cause poor fits when they are absent from the basis set. It might still be possible to include some in the basis set, but the accuracy of their concentrations would generally correspond to the lower part of Table 1. One exception is

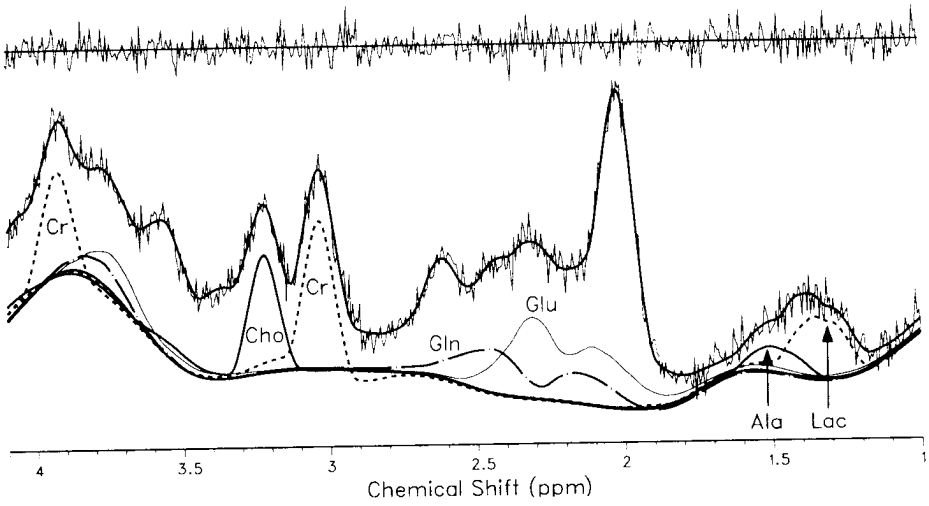

FIG. 4. LCModel analysis of a spectrum with poor resolution (FWHM = 0.11 ppm). Curve conventions are as in Fig. 2. The contribution of baseline plus total Cr+PCr is labeled Cr.

ethanol; in uptake experiments, it was added to the basis set and could be precisely estimated.

Data Requirements

LCModel is robust to noise, with the uncertainties in the concentrations remaining about proportional to the noise until quite high noise levels. The critical noise level is strongly dependent on the resolution. With the resolution in Figs. 1 and 2, good estimates should still be possible with twice the noise level in Fig. 1. However, in Fig. 4 the critical noise level has already been reached (except perhaps for NAA+NAAG, Cr+PCr, and Cho).

Lines should have a FWHM < 0.1 ppm. Ideally, FWHM ≈ 0.05 ppm, with 128 scans and a VOI ≥ 8 ml (as in Figs. 1 and 2), but metabolites high in Table 1 can still be reasonably well-estimated under less ideal conditions.

Important information is lost when the spectrum does not extend up to 4.0 ppm (preferably 4.1 ppm to get the *myo*-inositol peak in Fig. 1 or 4.2 ppm to also get solitary baseline). LCModel can account quite well for steeply rising or falling baselines due to incomplete water suppression, so only other severe artifacts prevent using data up to or beyond 4.0 ppm.

Computational Requirements

On the average, an LCModel analysis requires about 30 min on a VAX 4000–300 workstation. Newer faster processors, perhaps with compromises in the stringent default parameters for convergence and reliability in LCModel, might yield at least preliminary concentration estimates in a few minutes. This might allow real-time *in vivo* spectroscopy, where decisions on further measurements could be made while the patient was still in the machine. The computer program will be available.

Relaxation Times

The γ_i in Eq. [3] in the Appendix account for a different T_2 for each metabolite *in vivo*, but not for each proton in a metabolite. The resulting errors in the linewidths should be small compared with the total width, which is normally dominated by field inhomogeneities and accounted for by the lineshape coefficients, S_n.

Errors due to different T_1 times of protons within a metabolite are best avoided by using nearly fully relaxed *in vivo* spectra with $TR = 6$ s. Systematic errors with $TR = 3$ s are probably unimportant, except perhaps for Cr+PCr, which has strong resonances at 3.03 and 3.94 ppm that can have significantly different T_1 times (10).

Possible Improvements

The major limitation in localized proton MRS *in vivo* with short echo times is due to the baseline. Spectra with longer echo times have drastically reduced baseline distortions, but also less information. In principle, a global two-dimensional analysis with a series of spectra (and basis sets) with different echo times might yield much more accurate estimates for the lower part of Table 1. It could also improve the separation of metabolites with highly correlated spectra, such as glycine and *myo*-inositol. However, the uncertainties in the T_2 times *in vivo* would complicate the analysis and weaken the advantages.

Water suppression might be avoided with better analog-to-digital converters. The baseline could then be constrained to be non-negative, and the real and imaginary parts (with no zero-filling) could be constrained to be Hilbert transform pairs (11). The metabolite/water ratios might also be useful concentration measures. However, these advantages might be outweighed by the need to accurately account for the complicated T_2 distributions in the huge water signals, although these distributions themselves might yield useful information (12).

CONCLUSIONS

LCModel can estimate concentrations of even minor metabolites to high internal precision. This should be useful in physiological and clinical studies, particularly since the results are user-independent, with no subjective interaction. Numerous pathological cases can be reliably detected. Under typically varying conditions *in vivo*, concentrations relative to Cr+PCr are generally more accurate than absolute concentrations.

LCModel is robust to noise, poor resolution, and baseline distortions (including incomplete water suppression). However, regardless of the data analysis method used, fundamental uniqueness problems arise if the spectrum does not satisfy some minumum requirements on signal/noise and resolution. LCModel's estimated uncertainties in the metabolite concentrations are lower bounds (6), but they are still extremely useful and indispensible guides in assessing the reliability of the concentration estimates.

APPENDIX

Model

Both the *in vivo* data and the *in vitro* basis set are zero-filled to double the number of points in the time-domain and Fourier transformed. For clarity, the discrete Fourier transform vectors are written explicitly as functions of time, t, (in lower case) and frequency, ν, (in upper case). Thus, the *in vivo* pair is $y(t)$ and $Y(\nu)$. The discrete spectrum data points, $Y(\nu_k)$, are modeled as

$$\hat{Y}(\nu_k) = \exp[-i(\phi_0 + \nu_k\phi_1)]\left[\sum_{j=1}^{N_B}\beta_j B_j(\nu_k) + \sum_{i=1}^{N_M} C_i \sum_{n=-N_S}^{N_S} S_n M_i(\nu_{k-n};\gamma_i,\epsilon_i)\right], \quad [1]$$

with the constraints

$$C_i \geq 0, \qquad \gamma_i \geq 0, \qquad \sum_{n=-N_S}^{N_S} S_n = 1. \quad [2]$$

The C_i are the concentrations of the N_M metabolites. The N_M metabolite spectra in the *in vitro* basis set, $M_i(\nu;0,0)$, are broadened with the parameters γ_i (to account for shorter T_2 times *in vivo*) and shifted with the parameters ϵ_i (to account for small errors in referencing the spectra),

$$M_i(\nu;\gamma_i,\epsilon_i) = \mathcal{F}\{m_i(t)\exp[-(\gamma_i + i\epsilon_i)t]\}, \quad [3]$$

where $\mathcal{F}$ denotes the (Fast) discrete Fourier transform (FFT), and $m_i(t)$ is the inverse FFT of the model spectrum $M_i(\nu;0,0)$. The last sum in Eq. [1] is a finite discrete convolution to account for field inhomogeneities, eddy currents, etc. with the lineshape coefficients S_n. The baseline is represented by N_B cubic B-splines, $B_j(\nu)$, with equally spaced knots. N_B and N_S are specified below. The zero- and first-order phase corrections are ϕ_0 and ϕ_1.

Regularization

A Marquardt modification (13) of a constrained Gauss-Newton least-squares analysis using the criterion

$$\frac{1}{\sigma^2(Y)}\sum_{k=1}^{N}\{\mathrm{Re}[Y(\nu_k) - \hat{Y}(\nu_k)]\}^2 + \|\alpha_S R_S \mathbf{S}\|^2 + \|\alpha_B R_B \boldsymbol{\beta}\|^2 + \sum_{i=1}^{N_M}\left\{\frac{[\gamma_i - \gamma_i^0]^2}{\sigma^2(\gamma_i)} + \frac{\epsilon_i^2}{\sigma^2(\epsilon_i)}\right\} = \text{minimum} \quad [4]$$

determines the concentrations, C_i, as well as ϕ_0, ϕ_1, γ_i, ϵ_i, $\boldsymbol{\beta}$ (the vector of the β_j), and $\mathbf{S}$ (the vector of the S_n). The first term in Eq. [4] is the usual least-squares criterion for the real part of the spectrum, $\mathrm{Re}[Y(\nu)]$. Typically, data are used from $\nu_1 = 4.1$ ppm to $\nu_N = 1.0$ ppm, and $N = 537$. The SD of the noise, $\sigma(Y)$, is estimated from the SD of a preliminary fit with $\alpha_S = \alpha_B = 0$ in Eq. [4].

The regularizor matrix, R_S, is given in Eq. (3.12) of ref. 6, except that the equality constraint in Eq. [2] is accounted for. The regularizor imposes smoothness and zero boundary conditions on the lineshape coefficients, S_n. The $\|\bullet\|$ is the Euclidean norm.

R_B, the smoothing regularizor matrix for the B-spline baseline, is specified in ref. 6, except that Eq. (3.13) should read

$$G_{jk} = \int_{\nu_1}^{\nu_N} B''_j(\nu)B''_k(\nu)\,d\nu, \quad [5]$$

where prime denotes differentiation. Knots 2 and $N_B - 1$ are at ν_1 and ν_N. Thus, one extra knot is outside of each boundary, and no boundary conditions are imposed.

In an inner loop, the regularization parameters, α_S and α_B, are increased with a constant α_S/α_B ratio until the boundary of the 50% confidence region for the fit to the data is reached (6). In the outer loop α_S/α_B is adjusted so that in Eq. [4] the penalties/degree of freedom are about equally weighted,

$$\|\alpha_S R_S \mathbf{S}\|^2/(2N_S) = \|\alpha_B R_B \boldsymbol{\beta}\|^2/N_B. \quad [6]$$

If this leads to lineshape coefficients, S_n, that form a unimodal peak with only two inflection points, then α_S/α_B is reduced (and the inner loop executed) as long as this condition holds.

The last terms in Eq. [4] represent prior normal probability distributions for the γ_i and ϵ_i. All the default expectation values, γ_i^0, correspond to a 2 s^{-1} increase in $1/T_2$ from *in vitro* to *in vivo* (10). All the $\sigma(\gamma_i)$ correspond to a 1 s^{-1} SD in $1/T_2$. All the $\sigma(\epsilon_i)$ correspond to a 0.004 ppm SD in the shifts, except for 0.002 ppm for NAA and NAAG (to prevent them from strongly overlapping) and 0.006 ppm for Cho (because of the variety of choline-containing metabolites). These default values were used for all analyses. These priors are mainly for stabilization when the search starts far from the minimum or when a metabolite has nearly zero concentration.

At each iteration in the least-squares analysis, the constraints in Eq. [2] result in a quadratic programming problem, which is solved with stable numerical methods (6). The β_j and C_i occur linearly, and separability (14) is exploited. The regularization, priors, and a maximum allowable step size further stabilize the problem. Analytical derivatives are used for all parameters.

Approximate Referencing, N_B, and N_S

The regularization automatically optimizes the effective number of degrees of freedom (6) in the baseline and lineshape. Thus, in principle, the results are independent of N_B and N_S as long as they are large enough to represent the baseline and lineshape to within experimental error. In practice, the following economic choices of N_B and N_S improve the rate of convergence in Eq. [4] and save computer time.

The *in vivo* spectrum, $Y(\nu)$, is initially referenced by cross-correlating the smoothed power spectrum of $y(t)$ with a sum of unit delta functions with default reference positions at 2.01, 3.03, and 3.22 ppm. After correction for the smoothing, the FWHM of this cross-correlation function is a measure of the spectral linewidth and is used to set N_B and N_S as follows: In Eq. [1], N_B is chosen so that the spacing between knots is the maximum of $\rho_B \times$ FWHM and 0.1 ppm. Similarly, N_S is chosen so that the finite convolution extends over $\rho_S \times$ FWHM, with $\rho_S = \rho_B = 1.5$ by default. These default values were used for all analyses. In about 1% of the cases, it was obviously necessary to rerun with extra input to change some defaults, e.g., with the Lac doublet as reference for cerebrospinal fluid when the default reference peaks were weak, or with $\rho_S = 2.5$ in the extreme case in Figs. 3A and 3B.

Except for initial referencing, the unsmoothed $Y(\nu)$ data are used. Smoothing destroys information and invalidates the criterion for choosing α_S and α_B (6). Similarly, no windowing is done. Exactly the same FFT is performed on the model in Eq. [3] and the data, to which the model is fit. Thus, any truncation effects are automatically accounted for, at least if the γ_i are approximately correct. However, to avoid an unnecessary loss of information, the time range should be long enough so that the *in vivo* time-domain data always decay into the noise.

ACKNOWLEDGMENTS

All spectra had been acquired and were run with LCModel by the Biomedizinische NMR Group at Max-Planck-Institut für biophysikalische Chemie. The author thanks J. Frahm for permission to use the examples in this paper and W. Hänicke, T. Michaelis, and K. D. Merboldt for helpful comments. Some of the computations were performed on the VAX 9000 at the Gesellschaft für wissenschaftliche Datenverarbeitung mbH, Göttingen.

REFERENCES

1. J. Frahm, T. Michaelis, K. D. Merboldt, H. Bruhn, M. L. Gyngell, W. Hänicke, *J. Magn. Reson.* **90,** 464 (1990).
2. T. Michaelis, K. D. Merboldt, W. Hänicke, M. L. Gyngell, H. Bruhn, J. Frahm, *NMR Biomed.* **4,** 90 (1991).
3. A. A. de Graaf, W. M. M. J. Bovée, *Magn. Reson. Med.* **15,** 305 (1990).
4. S. W. Provencher, T. Michaelis, W. Hänicke, J. Frahm, *in* "Works-in-Progress, 11th Annual Meeting, Society of Magnetic Resonance in Medicine, Berlin, 1992," p. 670.
5. S. W. Provencher, J. Glöckner, *Biochemistry* **20,** 33 (1981).
6. S. W. Provencher, *Comput. Phys. Commun.* **27,** 213 (1982).
7. T. Michaelis, K. D. Merboldt, H. Bruhn, W. Hänicke, J. Frahm, *Radiology* **187,** 219 (1993).
8. R. J. Ordidge, I. D. Cresshull, *J. Magn. Reson.* **69,** 151 (1986).
9. U. Klose, *Magn. Reson. Med.* **14,** 26 (1990).
10. J. Frahm, H. Bruhn, M. L. Gyngell, K. D. Merboldt, W. Hänicke, R. Sauter, *Magn. Reson. Med.* **11,** 47 (1989).
11. E. Bartholdi, R. R. Ernst, *J. Magn. Reson.* **11,** 9 (1973).
12. R. M. Krocker, C. A. Stewart, M. J. Bronskill, R. M. Henkelman, *Magn. Reson. Med.* **6,** 24 (1988).
13. D. W. Marquardt, *J. Soc. Indust. Appl. Math.* **11,** 431 (1963).
14. G. H. Golub, V. Pereyra, *Soc. Indust. Appl. Math. J. Numer. Anal.* **10,** 413 (1973).